Nanoscale

Accepted Manuscript

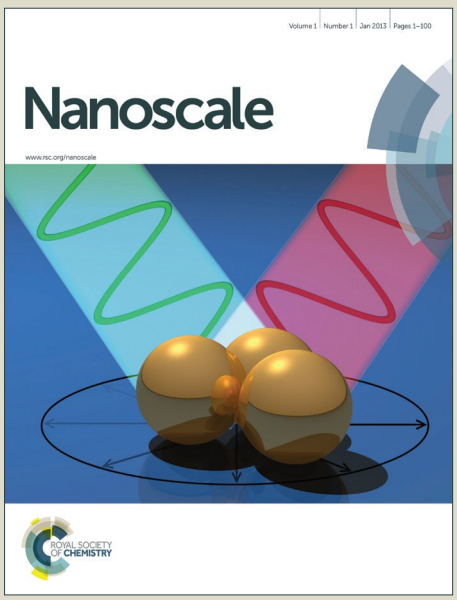

ROYAL SOCIETY OF CHEMISTRY

www.rsc.org/nanoscale

One-step fabrication of gold nanoparticles/carbon nanosheets hybrid by sonoelectrochemical technique for efficient surface-enhanced Raman scattering

Kaige Zhang, Su Yao, Gongke Li*, Yuling Hu*

School of Chemistry and Chemical Engineering, Sun Yat-sen University, Guangzhou, 510275, P.R. China

* Corresponding author: Gongke Li, Yuling Hu

Tel. : +86-20-84110922

Fax : +86-20-84115107

E. mail : cesgkl@mail.sysu.edu.cn

ceshyl@mail.sysu.edu.cn.

Abstract

A simple, fast, reproducible and efficient one-step fabrication method was successfully developed to prepare gold nanoparticles/carbon nanosheets hybrids (Au NPs/CNS) by sonoelectrochemical technique. This method involved simultaneous generation of carbon nanosheets (CNS) by oxidation of graphite anode and Au NPs by reduction of $AuCl_4^-$ on the surface of cathode. Then the Au NPs modified with poly(diallyl dimethyl ammonium chloride) were self-assembled on the surface of CNS. A homemade sonoelectrochemical device which can provide both high electric field and ultrasonic filed was applied. Benefit from the synergy effect of electric field and ultrasonic field, Au NPs with controlled size and distribution on the surface of CNS could be obtained, which exhibited high-quality and distinctive SERS activity. The enhancement factor of the developed substrate was 1.2×10^6 using 4-aminothiophenol as the probe molecule. Taking advantage of the high affinity of CNS toward aromatic molecules and the SERS activity of Au NPs, Au NPs/CNS showed a great increase of Raman signals for aromatic molecules. The SERS substrate also showed the charge selectivity to the cationic aromatic dyes, due to the negative charge on the surface of CNS. Subsequently, the potential practical application of the SERS substrate was evaluated by quantitative analysis of adenine. The results foresee the Au NPs/CNS nanomaterials as sensitive SERS-active substrates having great potential for detection of biomolecules.

Keywords: One-step fabrication, gold nanoparticles/carbon nanosheets, sonoelectrochemical technique, surface-enhanced Raman scattering.

Introduction

Surface-enhanced Raman spectroscopy (SERS), as an ultra-sensitive and powerful analytical technique for molecular sensing and detection, has received increasing attention.[1-4] It has been generally accepted that the large enhancement of normally weak Raman signals arises from an electromagnetic mechanism and a chemical mechanism. Electromagnetic mechanism is based on the enhancement of the local electromagnetic fields generated at or near nanostructured surfaces, while chemical mechanism is based on the physical or chemical adsorption of the analyte to metal surface to produce charge-transfer states between adsorbed molecules and metal surface.[5-8] In this sense, both the electromagnetic mechanism and chemical mechanism enhancement require a close proximity of the analyte toward the metal surface.

However, the adsorption ability of analyte on the surface of the metal nanoparticles has a strong relation with their molecular structures. Hence the poor affinity of the molecules toward the metal surface restricted direct analysis of diverse molecules. To address this issue, various approaches have been proposed to improve affinity of the analyte to the surface of metal nanoparticles[9-15], such as removing the undesired capping agents for SERS, the functionalization of nanoparticles by different surface function groups, exploiting the mechanical trapping, and conversion of the analytes by derivatization reaction. Nevertheless, the fixed functional molecules make them only trap organic molecules who have strong interaction with functional molecules. Recently, many researchers focus on fabricating metal nanoparticles (MNPs) on the surface of carbon nanomaterials (e.g. carbon nanotube[16-18], graphene[19-21] and graphene oxide[22-26]), which have exhibited fascinating potential in the SERS analysis of diverse target molecules due to its high affinity to these compounds. These

carbon nanomaterials with high specific large surface area had been used as effective absorbent for aromatic molecules through electrostatic bonding or π-π cooperative interaction.[26] In addition, these carbon nanomaterials, which were functionalized by different functional reagents, showed potential in selective trap of the target analytes. [23] So, we believe that this kind of hybrids may serve as a useful tool to trap target molecules with poor affinity toward the metal surface and thus to provide strong SERS signals.

To apply SERS in routine studies for molecular detection, SERS-active substrate should be reproducible, inexpensive and easy to be fabricated. Up to now, there have been two common approaches for the hybridization of carbon nanomaterials and MNPs: (1) reduction of the metal ionic precursor along with simultaneous deposition of resultant MNPs on the surface of carbon nanomaterials (*in situ* method),[20, 21, 26, 27] (2) dispersion of pre-synthesized MNPs in a carbon nanomaterials solution followed by the adsorption of MNPs on the surface of carbon nanomaterials (self-assembled method).[22,28-31] Hu *et al*[26] reported a direct growth of Au NPs on reduced graphene oxide (rGO) film. This method involved an anode oxidation of bulk Au as sacrificial anode to generate Au ion precursor, which was then reduced on the pre-fabricated rGO/polyethlene terephthalate film by the electric field. However, these carbon nanomaterials needed to be pre-synthesized in the above methods. Up to now, some carbon nanomaterials including graphene and graphene oxide was usually prepared through oxidative exfolication of graphite by modified Hummers'method[23, 24], which is time-consuming and complex. Recently, our group[32] developed a one-step sonoelectrochemical method for preparing the carbon nanoparticles in the pure water, which is rapid and facile. Our interest was to develop a facile and one-step strategy to prepare the hybrid of the carbon nanomaterials and noble metal.

In this paper, a facile one-step fabrication method was developed to fabricate sized-controlled gold nanoparticles/carbon nanosheets hybrid (Au NPs/CNS) by sonoelectrochemical technique. Carbon nanosheets (CNS) were generated by direct oxidation of graphite anode under the high intensity electric field. Simultaneously, Au NPs were generated by reduction of $AuCl_4^-$ ions on the cathode. Both components were dispersed into the electrolytic solution under ultrasonic field. Thereafter, Au NPs/CNS nanomaterials were formed by self-assembly of the Au NPs on the surface of CNS. To obtain this goal, a homemade sonoelectrochemical device providing both high intensity electric field and ultrasonic field was applied. Benefit from the synergy effect of electric field and ultrasonic field, the method was quite simple, fast, reproducible and efficient. The resultant hybrids were supposed to possess the combined properties of CNS and Au NPs, including the high affinity of CNS toward aromatic molecules and the localized surface plasmon resonance based SERS property of Au NPs. Furthermore, we show the potential of Au NPs/CNS nanomaterials for SERS detection of biomolecules.

Experimental

Sonoelectrochemical device

A homemade sonoelectrochemical device[32] reported in our previously published work was used to synthesize Au NPs/CNS hybrids. The scheme of the sonoelectrochemical device was shown in **SI Fig. 1**. The body of electrolyzer was made from polymethyl methacrylate. A spectrum pure graphite ring and a titanium tube were placed in the center of electrolyzer as anode and cathode respectively. The thin O-ring with a thickness of 2 mm was used to separate the anode and cathode. The ultrasonic generator was placed through the titanium tube cathode. The hollow shape

of cathode ensured that the ultrasonic power acted on the graphite anode. The hollow shape of the anode made the high intensity electric field almost uniform. The graphite anode's external diameter was 20 mm with its inner diameter and height of 12 and 15 mm respectively. This sonoelectrochemical device can provide the high intensity electric filed and ultrasonic filed.

Regents and apparatus

Polyvinylpyrrolidone (PVP, Mw ≈ 58, 000, K29-32), poly(diallyl dimethyl ammonium chloride) (PDDA, 35% wt in water, Mw < 100, 000), chloroauric acid ($HAuCl_4$), methylene blue (MB), crystal violet (CV), sunset yellow (SY), congo red (CR), anthracene (Ant), pyrene (Py) and 4-aminothiophenol (4-ATP) were purchased by Shanghai Jingchun Reagent Co., Ltd. (Shanghai, China). KNO_3 was brought from Sinopharm Group Chemical Reagent Co. Ltd. (Shanghai, China). Adenine, thymine, cytosine, uracil and guanine were purchased from Sigma (USA). Fish sperm and calf thymus DNA were obtained from Shanghai Chemical Co. Ltd. (Shanghai, China). Perchloric acid and sodium hydroxide were brought from Damao Chemical Reagent Factory (Tianjin, China). The all chemicals were analytical grade and used without any further treatment. Ultrapure water was used throughout the study.

A Zhaoxin KXN-3002D DC power source was used to provide the electrolytic voltage. A XinZhi JY92-□ultrasonic disruptor was used to provide the ultrasonic field. A battery-powered Raman spectrometer (model Inspector Raman, diode laser excitation wavelength λex¼785 nm) in the range 200-2200 cm^{-1} was used to provide the Raman spectra. This system consists of a liquid-N_2-cooled CCD detector (Model Spec-10:400B, Roper Scientific, Trenton, NJ) with a spectral resolution of 8 cm^{-1} and a data acquisition system (Photometrics, Tucson, AZ). Renishaw inVia Laser micro-Raman spectrometer with He/Ne laser excitation at 532 nm was also used to provide

the Raman spectra. A 100× objective was used to focus the laser beam and to collect the Raman signals. Ultraviolet-visible absorption spectra were performed on a Cary-100Conc UV-vis spectrophotometer (Varian, American). Zeta-potential measurements were performed by a Nanoparticle size-zeta potential and molecular weight analyzer (Brookhaven, American). Transmission electron microscopy (TEM) characterization was performed on a PHILIPS TECNAI 10 TEM instrument (Philips, Netherlands). X-ray diffractomery (XRD) was carried out using a RIGAKU diffractiometer. X-ray photoelectron spectroscopy (XPS) experiments were performed on an ESCA LAB 250 XPS instrument, which was equipped with the Mono AlKα X-ray radiation as the source for excitation at a pressure of less than 2×10^{-9} mbar in the chamber. Infrared absorption spectra were performed on a NICOLET AVATAR 330 Fourier transform infrared (FT-IR) spectrometer.

One-step fabrication method of Au NPs/CNS hybrid

The synthesis of Au NPs/CNS was performed in a homemade sonoelectrochemical device mentioned above. The electrolytic solutions were consisted of KNO_3 (50 mmol L^{-1}), PDDA (0.05%, wt) and $HAuCl_4$ (0.05%, wt). PDDA served as chemical functional agent to modify Au NPs and connect Au NPs with CNS. The electrolysis was carried out in a constant current at 100 mA. The ultrasonic power was 40 W. After ultrasonic electrolysis for 5 min, the Au NPs/CNS was obtained.

In the control experiment, Au NPs and CNS were also synthesized respectively by the sonoelectrochemical method. In detail, Au NPs were prepared in a similar way except that graphite electrode was replaced by Au electrode as anode. CNS was also prepared in the similar way except that $HAuCl_4$ was not added to electrolytic

solutions. The other reaction conditions were the same as the synthesis of Au NPs/CNS.

SERS experiments

For preparation of SERS substrates, the silicon substrate was first washed by ultrasonication in acetone, ethanol, and water in turn. Then the substrate was treated in Piranhasolution (98%H_2SO_4/30%H_2O_2=3:1, v/v; *CAUTION:* piranha solution should be handled with great care) to clean the organic compounds and provide a hydroxylated surface. Au NPs, CNS or Au NPs/CNS were then deposited on the surface of the silicon substrate by simple drop-casting.[33] The number of the adsorbed dye molecules on the substrate may not well control by solution soaking method. One way to overcome this difficulty was to employ vacuum deposition.[29, 34] To ensure the comparable substrates with the same target molecules, 10 μL of CV, MB, Ant, Py, SY or CR solution with the same concentration (10^{-6} mol L^{-1}) were dropped onto the substrate respectively and dried by vacuum evaporation to ensure an equal distribution. Raman spectra of the samples were measured by a portable Raman spectrometer equipped with wavelength of 785 nm and a power of 30 mW with the range 200-2200 cm^{-1}. The typical exposure time for each measurement in this study was 1s with five accumulations unless specified.

Result and discussion

Fabrication of Au NPs/CNS

One-step sonoelectrochemical technique was used to fabricate Au NPs/CNS. The schematic illustration of fabrication was shown in **Fig. 1**. Generally, the CNS was generated by oxidation of graphite anode under the high intensity electric field.

198 Simultaneously, Au NPs were produced by reduction of $AuCl_4^-$ ions on the surface of
199 titanium cathode. Afterwards, the resultant CNS and Au NPs modified with PDDA
200 were dispersed into the electrolytic solution under ultrasonic field. At the same time,
201 Au NPs/CNS nanomaterials were acquired by self-assembling Au NPs on the surface
202 of CNS. This synthetic strategy possesses several superiorities over the previous
203 method. Firstly, the fabrication of the Au NPs/CNS hybrid can be accomplished in a
204 one-step procedure, which simplifies the operation and facilitates the synthetic
205 efficiency. Secondly, the fabrication is completely "green" and no toxic reagents or
206 solvents are required. Thirdly, highly dispersive and homogenous attachment of Au
207 NPs on the surface of CNS owing to the synergy effect of electric field and ultrasonic
208 filed as compared with other synthetic strategies.
209
210 **Fig.1**

211 During the procedure of formation of Au NPs/CNS, the modifier plays an
212 important role. At the beginning of the experiment, we attempted to synthesize the Au
213 NPs/CNS without adding any chemical functional agent. However, this would lead to
214 the deposition of Au NPs on the surface of titanium cathode instead of dispersion in
215 the electrolytic solution. To solve this problem, the use of chemical functional agent is
216 needed to prevent the Au NPs depositing on the surface of titanium cathode. PVP[35]
217 was the commonly used stabilizing agent for Au NPs due to its unique chemical
218 structure and properties. But to our surprise, the Au NPs was dispersive in electrolytic
219 solution but not self-assembled on the surface of CNS by using PVP as modifier.
220 PDDA is a kind of cation polyelectrolyte which can usually act as stabilizing agent in
221 the synthesis of colloids[36] and a chemical functional agent[37]. In order to achieve the
222 Au NPs/CNS, PDDA was chosen as chemical functionalized agent in our study owing

to the following reasons. PDDA is good candidate as modifier to stabilize the Au NPs. Au NPs modified with PDDA exhibited positive charges, and can be self-assembled on the surface of CNS with negative charges by electrostatic adsorption. The concentration of PDDA had an impact on the generation and SERS activity of Au NPs/CNS. When the concentration of PDDA was less than 0.05%, Au NPs cannot be completely dispersed. The stable Au NPs/CNS nanomaterials were formed until the concentration of PDDA was above 0.05%. Excess PDDA had negative effect to the SERS performance of Au NPs/CNS (**SI Fig. 2**). Therefore, the concentration of the PDDA was optimized to 0.05%.

Ultrasonic field plays a crucial role in the fabrication of Au NPs/CNS. The Au NPs and CNS formed must be rapidly transferred from the cathode and anode vicinity to the bulk solution, thus to facilitate the self-assembly of Au NPs on the surface of CNS. If the fabrication of the Au NPs/CNS was carried out without ultrasonic field, deposition of Au NPs and CNS on the respective electrode would occur. Other conditions that affected the fabrication and SERS of Au NPs/CNS were also investigated (**SI Fig. 2 and SI Fig.3**). The size and density of Au NPs on the CNS, and Raman activity of Au/CNS were depended strongly on the concentration of $HAuCl_4$. When the concentration of $HAuCl_4$ was 0.05%, the best SERS signal can be obtained. The concentration of KNO_3 (50 mmol L^{-1}), ultrasonic power (40 W), electric current (100 mA) and electrolytic time (5 min) were used for generating high SERS active Au NPs/CNS substrate.

Characterization of Au NPs/CNS

The morphology and structure of CNS and Au NPs/CNS were first examined by TEM (**Fig. 2 A and Fig. 2B**). The TEM image of the CNS clearly illustrated the flake-like shape with some corrugations. The TEM of Au NPs/CNS showed that

roughly spherical Au NPs with diameters of 56.0±10.1 nm were attached on the surface of CNS. Furthermore, the presence of Au element in the hybrids was confirmed by the XPS. As shown in **Fig. 2C**, the XPS revealed that Au NPs/CNS consisted of the elements of C, O, Au and N. The signals of C and O originated from CNS. The presence of Au element in Au NPs/CNS confirmed the successful decoration of CNS with Au NPs. The existence of N element was supposed to be induced by PDDA modifier. Large number of C=C and C-C existed on the surface of CNS and Au NPs/CNS (**Fig.2 E and Fig.2F**), which showed the potential of Au NPs/CNS to adsorbed target analytes by π–π interaction.[23,28] The result of XPS and FT-IR (**SI Fig.4**) exhibited that abundant of carboxyl groups existed on the surface of CNS. The zeta potentials (ζ) of the as-synthesized CNS were -35 mV, which further proved that large amounts of negative charges were present on the surface of CNS. On the other hand, as shown in **Fig. 2D**, the Au 4f for Au NPs/CNS can be detected and the binding energy of 83.6 eV for Au $4f_{7/2}$ state and 87.2 eV for Au $4f_{5/2}$ state are identified respectively.

Fig.2

UV-vis absorption spectra of aqueous dispersion of CNS and Au NPs/CNS were shown in **Fig. 3A**. After decoration with Au NPs on the surface of CNS, there was evidently a new peak at about 543 nm. This was the characteristic of Au NPs due to the surface plasmon absorption, which implied Au NPs attaching on the surface of CNS. XRD was also used to verify the formation of Au NPs/CNS. As shown in **Fig. 3B**, four peaks were observed at 2θ= 38.187, 44.385, 64.576 and 77.567, which can be indexed to the (111), (200), (220) and (311) reflections of metal gold, respectively

(JCPDS No. 65-2870). The result indicated that Au NPs had been successfully self-assembled on the surface of CNS.

Raman spectrum of carbon nanomaterials[17, 19-21, 23, 26, 38] usually exhibited the regular two peaks, corresponding to the D-band line (1350 cm^{-1}) and the G-band line (1580 cm^{-1}). The D-band at 1352 cm^{-1} is a disorder-activated Raman mode that indicates extensive oxidation of the graphite, whereas the G-band centered at 1595 cm^{-1} is characteristic of the sp^2-hybridized carbon atoms in the hexagonal framework, which is important for the adsorption of molecules through nonconvalent interaction. With decoration of Au NPs, the intensity of the D and G bands of CNS obviously increase by 503% and 506% respectively in comparison with those of the CNS under the same test conditions (**Fig. 3C**), which could be attributed to the coupled surface plasmon resonance absorption of the Au NPs on the CNS.

Fig. 3

SERS properties

The as-prepared Au NPs/CNS nanomaterials were used as efficient SERS substrate for organic molecule sensing. The Raman signals of the model molecules on bare silicon, CNS, Au NPs and Au NPs/CNS substrates were measured and compared under the same conditions (integration time, laser power, focus, etc.). In this case, CV and MB (positively charged molecule), Ant and Py (neutral molecule), SY and CR (negatively charged molecule) were used as model probe molecules. For the above six molecules, the SERS spectra obtained from the Au NPs/CNS were more intense than those from Au NPs (**Fig.4**). These observations indicated that CNS modification indeed amplified the SERS signals of the six model molecules. It is supposed to be

strong interaction between CNS and the aromatic molecules because of the π–π electrostatic stacking properties originated in GO material.[29, 39]

Fig.4

The enhancement effect of CNS was quantitatively analyzed by applying SERS intensity ratio (n) between the Au NPs/CNS and Au NPs substrates, and described by the following equation: $n=I_{di}/I_{ci}$.[23] As schematically shown in **Fig.4**, I_{di} and I_{ci} were the intensity of Raman shift (*i*) obtained on the Au NPs/CNS and Au NPs, respectively. The SERS intensity ratios and the assignment of the Raman bands of the four Raman probe molecules were summarized and compared in **Table. 1**. Obviously, the enhancement effect of the Au NPs/CNS to probe molecules from high to low were positively charged molecules, neutral molecule and negatively charged molecules in turn. This phenomenon can be rationalized by different affinity of the Au NPs/CNS to the different kinds of molecules. In detail, negatively charged CNS had strong electrostatic attraction with model molecules by the π-π interaction and charge interaction, which enabled the direct adsorption of these molecules near the metal surface thus gave high SERS enhancement. On the other hand, Au NPs modified with PDDA can drive easily negatively charged molecules on their surfaces. According to above results, negatively charged CNS played more important role than Au NPs modified with positively charged PDDA on the adsorption molecules to the surface of Au NPs/CNS. The charge tendency of the Au NPs/CNS would benefit to improve SERS selectivity.

Table 1

On the basis of the above results, we propose that the driving force of the mainly effects of CNS on the SERS intensity is dictated by strong adsorption of analytes both by π-π interaction and charge interaction.

For quantitative detection, it is very important for SERS substrates to have good uniformity and reproducibility. It was reported that a substrate with poor uniformity and reproducibility would lead to Raman intensity different of 2-3 times from one spot to another.[23] Consequently, the uniformity and reproducibility of Au NPs/CNS as SERS substrate were evaluated using 4-ATP as the probes molecules. We checked the reproducibility of the SERS measurement by recording spectra from the 40 randomly selected places on the same batch and taking SERS spectra with 30 different batches of the samples. The relative stand deviations of the 1073 cm^{-1} were 9.9% and 12.9% respectively (**SI Fig. 5**), which indicated the Au NPs/CNS as SERS substrate had high uniformity and good reproducibility. Additionally, we estimated the enhancement ability of Au NPs/CNS substrate by calculating the enhancement factors (EF) of 4-ATP molecular. The EF was calculated to be 1.2×10^6 at 1073 cm^{-1} for the Au NPs/CNS (**SI Fig. 6**), which is comparable to other Au NPs decorated carbon nonmaterial hybrid SERS substrates.[20] However, this sonoelectrochemical method may offer a simple and effective way for fabrication hybrid of CNS and metal nanoparticles with controlled size and distribution.

SERS detection of adenine

Adenine plays a significant role in biological system as it has widespread effect to coronary and cerebral circulation, energy transduction, enzymatic reactions as cofactors, and even in cell signaling.[45, 46] Abnormal changes of its concentration may indicate the presence of various diseases. Therefore, quantification of adenine is

critical for the investigation of a wide variety of biological issues. Adenine can be protonated in acid and deprotonated in base (**SI Fig.7**). As shown in **Fig. 5A**, the SERS of adenine at pH 4.00 was 1.34 times of that at pH 11.00. This result can be explained that CNS had more adsorption of protonated adenine near the metal surface thus gave high SERS enhancement.

To examine the linear range in SERS detection of adenine, the pronounced and isolated band of adenine located at 734 cm^{-1} **(Fig. 5A**) was selected for quantitative detection. **Fig. 5B** shows the obtained concentration-response curve for adenine in aqueous solution at pH 4.00. Based on **Fig. 5B**, SERS signal of adenine increases as concentration of adenine and remains almost constant after 10 mg L^{-1}. The linear regression coefficient value is 0.9966 in the concentration range of 0.1-10.0 mg L^{-1}. The limit of detection was 0.04 mg L^{-1}.

Fig. 5

To examine the feasibility of the Au NPs/CNS in determination of adenine under interference of other nucleobases, adenine solutions (0.7 mg L^{-1}) were mixed with equimolar concentration of the other nucleic bases such as guanine, cytosine, thymine and uracil. The SERS intensity of adenine ring breathing mode at 734 cm^{-1} was used to determine the adenine under co-existing of second nucleobases. The results indicated that the investigated nucleic bases did not interfere the determination of adenine, since a variation of the Raman intensity at 734 cm^{-1} was less than ±5%. The result reveals a high selectivity for adenine determination.

The method was then applied to the analysis of adenine in acid hydrolyzate of the beer and DNA (fish sperm), respectively (**Fig. 6)**. The recoveries were evaluated by adding known amounts of standard adenine solution to the samples. The recoveries

varied from 82.4 to 94.2%, showing the excellent performance of the method for the examined samples (**Table 2**). To evaluate the proposed SERS method, the samples were also analyzed by HPLC.[47, 48] The results (**Table** 2) indicated that there was no significant difference between two methods. The result agreed well with the conventional HPLC method, suggesting the potential application for detection of biomolecules.

Fig. 6

Table 2

Conclusion:

In summary, we have illustrated a simple, fast, reproducible and efficient one-step strategy to fabricate Au NPs/CNS by sonoelectrochemical technique. The all process was finished in a homemade sonoelectrochemical device, which can provide the high intensity electric field and ultrasonic field. The electric and ultrasound field plays a crucial role in the production and dispersion of Au NPs and CNS. The as-prepared Au NPs/CNS nanomaterials combined the unique properties of Au NPs and CNS, and exhibited significantly SERS enhancement to aromatic molecules. The Au NPs/CNS as SERS substrate also showed the charge selectivity to the cationic aromatic dyes, due to role of the CNS nanomaterials with negatively charges. Significantly, the SERS substrate could produce highly enhanced Raman signals (EF~1.2×10^6) with good uniformity and reproducibility. Furthermore, Au NPs/CNS can be as an active SERS substrate for quantitative detection of adenine. These results foresee the Au NPs/CNS nanomaterials will have great potential as sensitive SERS-active substrates in routine studies for biomolecules. Considering the well-established sonoelectrochemical method in the preparation of nanomaterials, the present strategy

may also be applied in preparing other carbon nanomaterial based nanocomposites as well.

Acknowledgements

The work was supported by the National Natural Science Foundation of China (Nos.21277176 and 21127008) and Major National Scientific Instrument and Equipment Development Project (2011YQ03012409), respectively.

References

1 R. G. Freeman, K. C. Grabar, K. J. Allison, R. M. Bright, J. A. Davis, A. P. Guthrie, M. B. Hommer, M. A. Jackson, P. C. Smith, D. G. Walter and M. J. Natan, *Science*, 1995, **267**, 1629-1632.

2 K. Kneipp, Y. Wang, H. Kneipp, L. T. Perelman, I. Itzkan, R. R. Dasari and M. S. Feld, *Phys. Rev. Lett.*, 1997, **78**, 1666-1670.

3 S. Nie and S. R. Emory, *Science*, 1997, **275**, 1102-1106.

4 A. Campion and P. Kambhampati, *Chem. Soc. Rev.*, 1998, **27**, 241-250.

5 S. Schlücker, *ChemPhysChem*, 2009, **10**, 1344-1354.

6 J. R. Lombardi and R. L. Birke, *Accounts Chem. Res.*, 2009, **42**, 734-742.

7 X. M. Qian and S. M. Nie, *Chem. Soc. Rev.*, 2008, **37**, 912-920.

8 Y. J. Ye, H. L. Liu, L.B. Yang and J. H. Liu, *Nanoscale*, 2012, **4**, 6442-6448.

9 L. Guerrini, J. V. Garcia-Ramos, C. Domingo and S. Sanchez-Cortes, *Anal. Chem.*, 2009, **81**, 953-960.

10 L. Guerrini, J. V. Garcia-Ramos, C. Domingo and S. Sanchez-Cortes, *Anal. Chem.*, 2009, **81**, 1418-1425.

11 Y. F. Xie, X. Wang, X. X. Han, X. X. Xue, W. Ji, Z. H. Qi, J. Q. Liu, B. Zhao and Y. Ozaki, *Analyst*, 2010, **135**, 1389-1394.

12 A. D. Strickland and C. A. Batt, *Anal. Chem.*, 2009, **81**, 2895-2903.

13 R. A. Alvarez-Puebla and L. M. Liz-Marzán, *Chem. Soc. Rev.*, 2012, **41**, 43-51.

14 R. A. Alvarez-Puebla, L. M. Liz-Marzán and F. J. Garcıá De Abajo, *J. Phys. Chem. Lett.*, 2010, **1**, 2428-2434.

15 K.G. Zhang, Y.L.Hu and G.K. Li, *Talanta*, 2013, **116**, 712-718.

16 X. J. Wang, C. Wang, L. Cheng, S. T. Lee and Z. Liu, *J. Am. Chem. Soc.*, 2012, **134**, 7414-7422.
17 Y. C. Chen, R. J. Young, J. V. Macpherson and N. R. Wilson, *J. Phys. Chem. C*, 2007, **111**, 16167-16173.
18 H. Zhao, H. G. Fu, C. G. Tian, Z. Y. Ren and G. H. Tian, *J. Colloid Interf. Sci.*, 2010, **351**, 343-347.
19 X. Q. Fu, F. L. Bei, X. Wang, S. O'Brien and J. R. Lombardi, *Nanoscale*, 2010, **2**, 1461-1466.
20 S. T. Sun and P. Y. Wu, *Phys. Chem. Chem. Phys*., 2011, **13**, 21116-21120.
21 Z. Zhang, F. G. Xu, W. S. Yang, M. Y. Guo, X. D. Wang, B. L. Zhang and J. L. Tang, *Chem. Commun.*, 2011, **47**, 6440-6442.
22 J. Huang, L. M. Zhang, B. Chen, N. Ji, F. H. Chen, Y. Zhang and Z. J. Zhang, *Nanoscale*, 2010, **2**, 2733-2738.
23 X. J. Liu, L. Y. Cao, W. Song, K. L. Ai and L. H. Lu, *ACS Appl. Mater. Inter.*, 2011, **3**, 2944-2952.
24 W. Fan, Y. H. Lee, S. Pedireddy, Q. Zhang, T. X. Liu and X. Y. Ling, *Nanoscale*, 2014, **6**, 4843-4851.
25 A. Saha, S. Palmal and N. R. Jana, *Nanoscale*, 2012, **4**, 6649-6657.
26 Y. Hu, L. H. Lu, J. H. Liu and W. Chen, *J. Mater. Chem.*, 2012, **22**, 11994-12000.
27 C. Xu, X. Wang and J. W. Zhu, *J. Phys. Chem. C*, 2008, **112**, 19841-19845.
28 F. A. He, J. T. Fan, F. Song, L. M. Zhang and H. L. Chan, *Nanoscale*, 2011, **3**, 1182-1188.
29 C. F. Hu, J. H. Rong, J. H. Cui, Y. H. Yang, L. F. Yang, Y. L. Wang and Y. L. Liu, *Carbon*, 2013, **51**, 255-264.
30 L. L. Zhang, C. L. Jiang and Z. P. Zhang, *Nanoscale*, 2013, **5**, 3773-3779.
31 J. Huang, C. Zong, H. Shen, Y. H. Cao, B. Ren and Z. J. Zhang, *Nanoscale*, 2013, **5**, 10591-10598.
32 S. Yao, Y. F. Hu and G. K. Li, *Carbon*, 2014, **66**, 77-83.
33 D. Li, M. B. Muller, S. Gilje, R. B. Kaner and G. G. Wallace, *Nat. Nanotechnol.*, 2008, **3**, 101-105.
34 X. Ling, L. M. Xie, Y. Fang, H. Xu, H. L. Zhang, J. Kong, M. S. Dresselhaus, J. Zhang and Z. F. Liu, *Nano Lett.*, 2010, **10**, 553-561.
35 B. S. Yin, H. Y. Ma, S. Y. Wang and S. H. Chen, *J. Phys. Chem. B*, 2003, **107**, 8898-8904.
36 H. J. Chen, Y. L. Wang, Y. Z. Wang, S. J. Dong and E. K. Wang, *Polymer*, 2006, **47**, 763-766.
37 S. Y. Wang, X. Wang and S. P. Jiang, *Phys. Chem. Chem. Phys.*, 2011, **13**, 6883-6891.

38 H. Zhao, H. G. Fu, T. S. Zhao, L. Wang and T. X. Tan, *J. Colloid Interf. Sci.*, 2012, **375**, 30-34.
39 Q. Su, S. P. Pang, V. Alijani, C. Li, X. L. Feng and K. Müllen, *Adv. Mater.*, 2009, **21**, 3191-3195.
40 X. X. Han, P. Pienpinijtham, B. Zhao and Y. Ozaki, *Anal. Chem.*, 2011, **83**, 8582-8588.
41 G. N. Xiao and S. Q. Man, *Chem. Phys. Lett.*, 2007, **447**, 305-309.
42 G. Lu, H. Li, C. Liusman, Z. Y. Yin, S. X. Wu and H. Zhang, *Chem. Sci.*, 2011, **2**, 1817-1821.
43 Y. F. Xie, Y. Li, L. Niu, H. Y. Wang, H. Qian and W. R. Yao, *Talanta*, 2012, **100**, 32-37.
44 Y.F. Xie, X. Wang, X.X. Han, X.X. Xue, W. Ji, Z.H. Qi, J.Q. Liu, B. Zhao and Y. Ozaki, *Analyst*, 2010, **135**, 1389-1394.
45 B. Kochanska, R. T. Smolenski and N. Knap, *Acta Biochim. Pol.*, 2000, **47**, 877-879.
46 A. Camilli and B. L. Bassler, *Science*, 2006, **311**, 1113-1116.
47 J. L. Gao, K. S. Leung, Y. T. Wang, C. M. Lai, S. P. Li, L. F. Hu, G. H. Lu, Z. H. Jiang and Z. L. Yu, *J. Pharm. Biomed. Anal.*, 2007, **44**, 807-811.
48 J. X. Shi, H. F. Liu, J. M. Wong, R. N. Huang, E. Jones and T. J. Carlson, *J. Pharm. Biomed. Anal.*, 2011, **56**, 778-784.

Table 1 SERS intensity ratio (n) and the assignments of several Raman bands of six Raman probe molecules

Probe molecules	Raman shift (cm^{-1})	n	Band assignment [23,40-44]
CV	915	5.0	ring skeletal vibration
	1177	4.6	ring C-H bending
	1613	4.5	ring C-C stretching
MB	673	5.9	out-of-plane C-H bending
	1397	6.0	in-plane ring C-H deformation
	1619	5.3	ring C-C stretching
Ant	1161	4.4	ring C-C stretching
	1403	4.5	ring C-C stretching/ring stretching
	1557	4.3	ring C-C stretching
Py	1237	4.0	ring C-C stretching/C-H in-plane bending
	1408	4.3	ring C-C stretching/ring stretching
	1620	3.9	ring C-C stretching
CR	1178	1.9	ring C-H bending
	1453	2.3	N=N stretching
	1591	1.9	ring C-C stretching
SY	1230	2.0	C-N stretching
	1391	3.2	in-plane ring C-H deformation
	1596	2.5	ring C-C stretching

The assignments of the peaks of CV, MB, Ant, Py, SY and CR are based on previous reports. [23,40-44]

Table 2 Determination of adenine in acid hydrolyzate of the DNA and beer by SERS and HPLC

sample	SERS				HPLC
	found[a,b]	Added	Recovery[a,b] (%)	RSD[c] (%)	found[a]
fish sperm	68.0	10.0	82.4	6.7	72.9 ± 6.4
DNA (mg g^{-1})		50.0	85.9	5.6	
calf thymus	44.1	10.0	90.2	6.8	40.1±3.5
DNA (mg g^{-1})		50.0	83.2	6.7	
beer 1 (mg L^{-1})	14.2	5.0	85.6	6.1	15.6± 0.9
		25.0	92.7	7.3	
beer 2 (mg L^{-1})	11.5	5.0	94.2	8.4	12.8±1.0
		25.0	85.0	7.3	

[a] Diluted appropriate times before analysis

[b] Quantitative date at 734 cm^{-1}.

[c] n=5, quantitative date from five different spots

Figure captions:

Fig.1 Schematic illustration of the fabrication of Au NPs/CNS by the one-step sonoelectrochemical method

Fig.2 TEM of (A) CNS and (B) Au NPs/CNS, (C) Survey XPS spectra of CNS and Au NPs/CNS, (D) Au4f XPS spectra of Au NPs/CNS, C1s XPS spectra of (E) CNS and (F) Au NPs/CNS

Fig. 3 (A) UV-Vis absorption spectra of (a) CNS and (b) Au NPs/CNS, (B) XRD of Au NPs/CNS, (C) Raman spectra of (a) CNS and (b) Au NPs/CNS

Fig.4 Raman spectra of CV, Ant, SY, MB, Py and CR (a) on silicon (the black line), (b) CNS (the red line), (c) Au NPs (the blue line) and (d) Au NPs/CNS (the green line). They were recorded under the same conditions where the concentration is 10^{-6} mol L^{-1}. Molecular structures of dyes are drawn inset. The excitation wavelength is 785 nm.

Fig. 5 (A) SERS of adenine (5 ppm) at different pH, (B) SERS intensity of adenine at 734 cm^{-1} from different concentration

Fig.6 (A) SERS of adenine from the beer spiked with 0 (a), 5.0 (b) and 25.0 (c) mg L^{-1}, (B) SERS of adenine from the fish sperm DNA spiked with 0 (a), 10.0 (b) and 50.0 (c) mg g^{-1} (diluted appropriate times before determination).

Fig.1

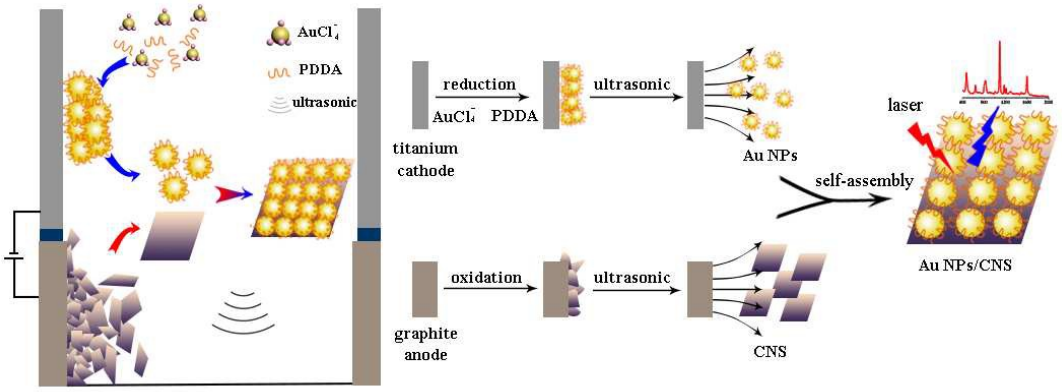

Fig.2

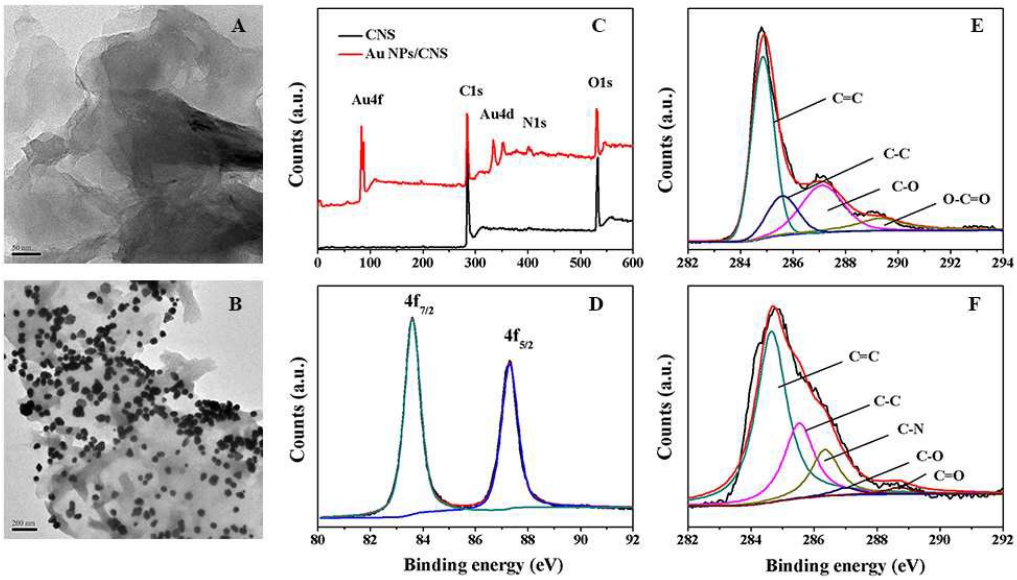

Fig.3

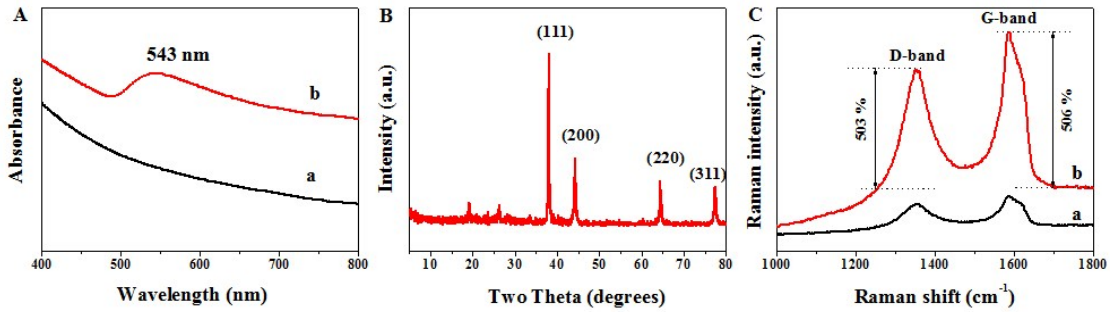

Fig.4

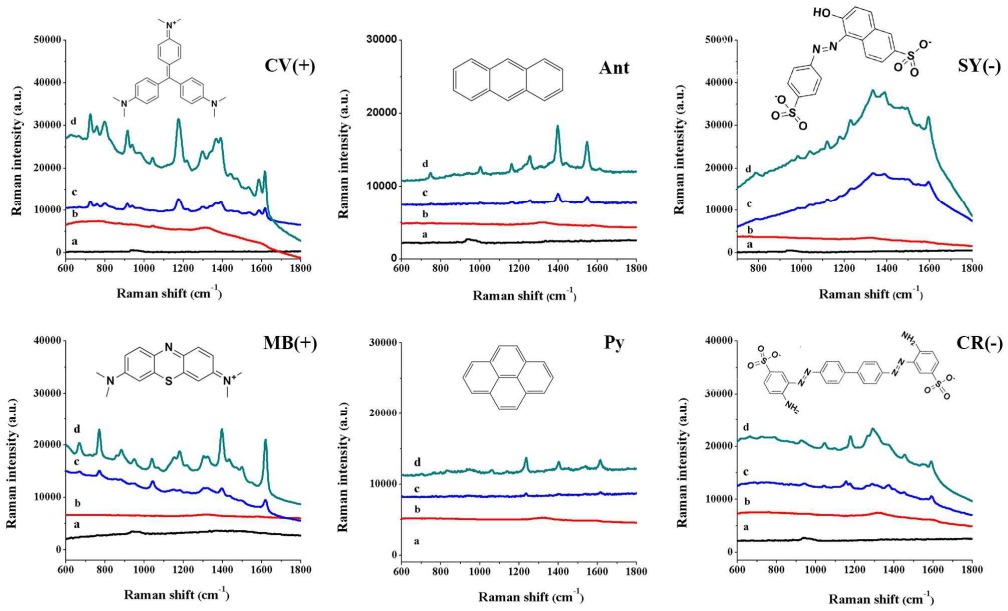

Fig.5

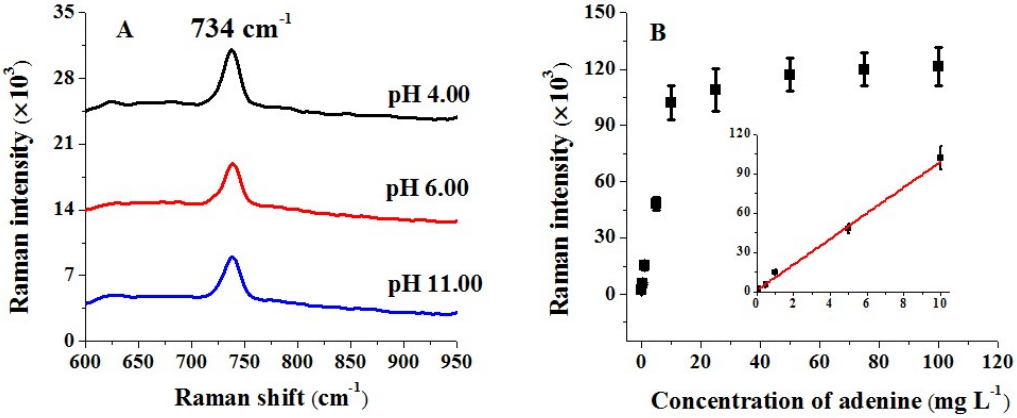

Fig.6